High-field superconductivity in alloyed MgB_2 thin films

V. Braccini,[1] A. Gurevich,[1] J. E. Giencke,[1] M. C. Jewell,[1] C. B. Eom,[1] D. C. Larbalestier,[1] A. Pogrebnyakov,[2] Y. Cui,[2] B. T. Liu,[2] Y. F. Hu,[2] J. M. Redwing,[2] Qi Li,[2] X. X. Xi,[2] R. K. Singh,[3] R. Gandikota,[3] J. Kim,[3] B. Wilkens,[3] N. Newman,[3] J. Rowell,[3] B. Moeckly,[4] V. Ferrando,[5] C. Tarantini,[5] D. Marré,[5] M. Putti,[5] C. Ferdeghini,[5] R. Vaglio,[6] and E. Haanappel[7]

[1]*Applied Superconductivity Center, University of Wisconsin-Madison, Madison, Wisconsin 53705, USA*

[2]*Pennsylvania State University, University Park, Pennsylvania 16802, USA*

[3]*Arizona State University, Tempe, Arizona 85287, USA*

[4]*Superconductor Technologies Inc., Sunnyvale, California 93111, USA*

[5]*University of Genoa/INFM-LAMIA, Genoa 16146, Italy*

[6]*University of Naples/INFM-Coherentia, Naples I-80125, Italy*

[7]*Laboratoire National des Champs Magnétiques Pulses, CNRS-UPS-INSA, Toulouse 31432, France*

(Received 15 September 2004; published 6 January 2005)

We investigated the effect of alloying on the upper critical field H_{c2} for 12 MgB_2 films, in which disorder was introduced by growth, carbon doping or He-ion irradiation, finding a significant H_{c2} enhancement in C-alloyed films, and an anomalous upward curvature of $H_{c2}(T)$. Record high values of $H_{c2}^{\perp}(4.2) \approx 35$ T and $H_{c2}^{\parallel}(4.2) \approx 51$ T were observed perpendicular and parallel to the *ab* plane, respectively. The temperature dependence of $H_{c2}(T)$ is described well by a theory of dirty two-gap superconductivity. Extrapolation of the experimental data to $T=0$ suggests that $H_{c2}^{\parallel}(0)$ may approach the paramagnetic limit of ~70 T.

DOI: 10.1103/PhysRevB.71.012504 PACS number(s): 74.70.Ad, 74.25.Op, 74.78.Db

Discovery of superconductivity in MgB_2 with the critical temperature $T_c = 39$ K renewed interest in the effects in two-gap superconductors. *Ab initio* calculations[1,2] showed that MgB_2 has two weakly coupled gaps $\Delta_\sigma(0) \approx 7.2$ meV and $\Delta_\pi(0) \approx 2.3$ meV residing on disconnected sheets of the Fermi surface formed by in-plane p_{xy} boron orbitals (σ band) and out-of-plane p_z boron orbitals (π band). The two-gap Eliashberg theory[2,3] has explained many anomalies in tunneling, heat capacity, and electrodynamics of clean MgB_2 single crystals.[4] However, the physics of two-gap MgB_2 alloys determined by the multiple impurity scattering channels, and by the complex substitutional chemistry of MgB_2 (Ref. 5) is still poorly understood. The behavior of disordered MgB_2 is particularly interesting because it exhibits enormous enhancement of H_{c2} by nonmagnetic impurities,[6–8] well above estimate $H_{c2}(0) = 0.69 T_c H'_{c2}(T_c)$ of one-gap theory,[9] and anomalous temperature-dependent H_{c2} anisotropy.[4] Some of these features have been explained by two-gap Usadel equations[10,11] in which impurity scattering is accounted for by the intraband electron diffusivities D_σ and D_π, and interband scattering rates $\Gamma_{\sigma\pi}$ and $\Gamma_{\pi\sigma}$. In this paper we address the fundamental question on how far can H_{c2} of MgB_2 be actualy increased by disorder. We present high-field transport measurements of $H_{c2}(T)$ for 12 MgB_2 films made by six experimental groups using very different ways of introducing disorder. We show that H_{c2} is radically increased in dirty films, and $H_{c2}^{\parallel}(0)$ extrapolated to $H_p \sim 70$ T for a C-alloyed film, comparable to the paramagnetic limit ($H_p = 1.84 T_c = 64$ T for $T_c = 35$ K).

Our films were made by different deposition techniques including pulsed laser deposition (PLD),[12,13] molecular beam epitaxy (MBE),[14] hybrid physical-chemical vapor deposition (HPCVD),[15] sputtering,[16,17] and reactive evaporation.[18] Growth was performed by *in situ*[14,15,17,18] and *ex situ* methods with post-annealing in Mg vapor.[12,13] C-doped films were produced by HPCVD[15] with the addition of 75 sccm of $(C_6H_7)_2Mg$ to the H_2 carrier gas.[19] Some films were damaged with 10^{16} cm^{-2}, 2 MeV α-particles to controllably alter the scattering by irradiation point defects.[20] Thickness and elemental compositions were determined by wavelength dispersive spectroscopy (WDS) and Rutherford backscattering spectroscopy (RBS), and film orientation and lattice parameters with a four-circle x-ray diffractometer. Film parameters are summarized in Table I. Thickness d of our films ranged from 105 to 245 nm, except film I with $d = 540$ nm. In some samples RBS detected through-thickness composition variations, likely due to surface reactions.

Measurements of $H_{c2}(T)$ on samples A,B,E,F,H,I,L were performed in a 33 T resistive magnet at the NHMFL in Tallahassee. Film resistance $R(H)$ were measured in parallel and perpendicular fields at a sweep rate of 1 T/min while temperature was stabilized to ~10 mK. The measuring current density J was varied between 10 and 100 A/cm^2. Detailed study of film A showed no significant change in $R(H)$ for $4 < J < 4000$ A/cm^2. Samples G, M and N were measured in the 300 ms 60 T pulsed facility at the LNCMP in Toulouse, at a lock-in frequency of 40 kHz and J varying from 50 to 200 A/cm^2 with no change in $R(H)$. In all cases H_{c2} was defined by $R(H_{c2}) = 0.9 R(T_c)$.

Figure 1 shows $H_{c2}^{\perp}(T)$ (a) and $H_{c2}^{\parallel}(T)$ (b) for the lower H_{c2} samples A,B,C,E,H,I,L,M,N. $R(H)$ curves for film A are shown in the inset. The $H_{c2}^{\perp}(T)$ data in Fig. 1(a) fall into two groups, one having $T_c \approx 32-37$ K, with relatively low H'_{c2} and $H_{c2}(0) \sim 10.5-15$ T, while the lower T_c group (24–32 K) has ≈50% larger H'_{c2} and $H_{c2}(0) \sim 17-22$ T. $H_{c2}(0)^{\parallel}$ data in Fig. 1(b) range from 18–40 T, with only samples B and L standing out. Film B, with the lowest $T_c \approx 24$ K and $H_{c2}(0)$ with $\rho_n \sim 85$ $\mu\Omega$ cm, has no anisotropy, while nontextured sample L with $\rho_n \sim 9.9$ $\mu\Omega$ cm also has a low $H_{c2}(0) \sim 22$ T in spite of its higher $T_c = 39.4$ K. Film E,

TABLE I. Sample list with texture and lattice parameters derived from XRD, and chemical compositions deduced from WDS. Impurities detected in amounts less than 1 at. % are not listed. ρ_n(40 K) was obtained from H_{c2} measurements (as-grown values are given in parentheses). $H_{c2}{}^{\parallel}$ and $H_{c2}{}^{\perp}$ values were extrapolated to 0 K, and g and D_π/D_σ were deduced from the fit of $H_{c2}(T)$ curves for all films. ($D_\pi/D_\sigma \ll 1$ means that the data point scatter does not allow us to distinguish between finite and zero D_π/D_σ, so the fit was performed for $D_\pi=0$.)

Samples	Substrate	T_c (K)	ρ_n(40 K) ($\mu\Omega$ cm)	$H_{c2}{}^{\perp}$ (T)	$H_{c2}{}^{\parallel}$ (T)	g	D_π/D_σ	c (Å)	a (Å)	Mg at. %	B at. %	C at. %	O at. %
A epitaxial[a]	(0001)Al_2O_3	35	9(4)	13.5	33	0.045	0.12	3.516	3.047	29	53	10	8
B fiber-textured[a]	(0001)Al_2O_3	23.7	86(56)	17	17	0.5	$\ll 1$			28	57	7	8
C epitaxial*[a]	(0001)Al_2O_3	34	7	20.5	30	0.06	$\ll 1$	3.52	3.08				
D fiber-textured*[b]	(111)$SrTiO_3$	31	220	33	48	0.075	$\ll 1$	3.547		37	32	14	17
E epitaxial	SiC	41.5	1.6(0.4)	12	34.5			3.511	3.107	30	57	2	11
F fiber-textured[c]	SiC	35	564	40	>74	0.045	$\ll 1$	3.542	3.117	26	46	21	6
G fiber-textured[c]	SiC	35	250	28.2	55.5	0.045	0.065	3.536	3.117	25	42	26	6
H epitaxial[c]	SiC	38	10.5	10.5	30	0.025	0.06	3.519	3.107	31	63	4	1
I untextured[d]	(0001)Al_2O_3	32	567(290)	21.7	26.8	0.09	0.08						
L no 00l textured[e]	r-cut Al_2O_3	39.4	9.9(2.8)	10.8	21.4	0.025	0.07			32	65	1	1
M epitaxial[f]	(111)MgO	33.5	47	14.6	38.1	0.095	0.1	3.533	3.036	24	41	28	6
N untextured[g]	(001)MgO	28.6	400	15.8	24.3	0.155	$\ll 1$			33	53	5	9

[a]Reference 16.
[b]Reference 13.
[c]Reference 15.
[d]Reference 14.
[e]Reference 18.
[f]Reference 12.
[g]Reference 17.

with highest $T_c=41.5$ K and $\rho_n \sim 0.4$ $\mu\Omega$ cm as made (1.6 $\mu\Omega$ cm when measured at the NHMFL) represents MgB_2 in the clean limit.[21] Although film *E* has the lowest ρ_n, it exhibits the highest $H_{c2}{}^{\parallel}(T)$, even though Fig. 1(b) also includes films with $\rho_n > 500$ $\mu\Omega$ cm but with lower $H_{c2}{}^{\parallel}$ (film *I*). Thus, there is no simple correlation between ρ_n and H_{c2}, because the global resistivity may be limited by poor intergrain connectivity[22] while H_{c2} is controlled by intragrain impurity scattering. The anisotropy parameter $\gamma(T) = H_{c2}{}^{\parallel}/H_{c2}{}^{\perp}$ ranges from ≈ 3 for the lowest ρ_n film *E* to ≈ 1 for the lowest T_c textured film *B*. For most films, $\gamma(T)$ tends to decrease as T decreases, consistent with the behavior predicted for two-gap MgB_2 with dirtier π band.[10]

Figure 2 shows $H_{c2}{}^{\parallel}(T)$ and $H_{c2}{}^{\perp}(T)$ curves for the highest H_{c2} films *F*, *G*, and *D*, while the insets show the parallel-field $R(H)$ traces. By increasing the nominal carbon content in the HPCVD films, resistivity rises from ~ 1.6 (*E*) to 564 (*F*) and 250 $\mu\Omega$ cm (*G*), while T_c only decreases to 35 K. However, $H_{c2}{}^{\perp}(0)$ increases from 12 T (*E*) to 28 (*G*) and ≈ 40 T (*F*). Furthermore, $H_{c2}{}^{\parallel}(0)$ rises from ≈ 35 T (*E*) to 51 T (*G*) and more than 70 T in sample *F*, while the anisotropy parameter $\gamma(T) = H_{c2}{}^{\parallel}(T)/H_{c2}{}^{\perp}(T)$ decreases as ρ_n increases. Figure 2(c) presents $H_{c2}(T)$ for sample *D*, made *ex situ* by PLD, which has high nominal O (17 at. %) and C (14 at. %) content[8] and shows $H_{c2}{}^{\perp}(0) \approx 33$ T and $H_{c2}{}^{\parallel}(0) \approx 48$ T.

The $H_{c2}(T)$ curves in Fig. 2 have an upward curvature inconsistent with the dirty limit one-gap theory.[9] For two-gap pairing, intraband scattering does not affect T_c, but T_c decreases as the interband scattering parameter $g=(\Gamma_{\sigma\pi}+\Gamma_{\pi\sigma})\hbar/2\pi k_B T_{c0}$ increases, where $T_{c0}=T_c(g=0)$. In MgB_2 g is small, and T_c does not change much, even if ρ_n is significantly increased.[23] The insensitivity of T_c to scattering makes it possible to increase H_{c2} in MgB_2 to a much greater extent than in one-gap superconductors by optimizing the diffusivity ratio D_π/D_σ, as follows from the equations for H_{c2} and T_c in a dirty two-gap superconductor[10]

$$2w(\ln t + U_+)(\ln t + U_-) + (\lambda_0 + \lambda_i)(\ln t + U_+) + (\lambda_0 - \lambda_i)(\ln t + U_-) = 0, \tag{1}$$

$$\psi\left(\frac{1}{2}+\frac{g}{t_c}\right) - \psi\left(\frac{1}{2}\right) = -\frac{2\ln t_c(w \ln t_c + \lambda_0)}{2w \ln t_c + \lambda_0 + \lambda_i}, \tag{2}$$

where $t=T/T_{c0}$, $t_c=T_c/T_{c0}$, $T_{c0}=T_c(g=0)$, $w=\lambda_{\sigma\sigma}\lambda_{\pi\pi}-\lambda_{\sigma\pi}\lambda_{\pi\sigma}$, $\lambda_0=(\lambda_-{}^2+4\lambda_{\sigma\pi}\lambda_{\pi\sigma})^{1/2}$, $\lambda_\pm=\lambda_{\sigma\sigma}\pm\lambda_{\pi\pi}$, λ_{mn} is 2×2 matrix of BCS coupling constants. Here $\lambda_i=[(\omega_- + \Gamma_-)\lambda_- - 2\lambda_{\sigma\pi}\Gamma_{\pi\sigma} - 2\lambda_{\pi\sigma}\Gamma_{\sigma\pi}]/\Omega_0$, $\Gamma_\pm=\Gamma_{\sigma\pi}\pm\Gamma_{\pi\sigma}$, $\omega_\pm = (D_\sigma \pm D_\pi)\pi H/\phi_0$, $\Omega_0=(\omega_-{}^2+\Gamma_+{}^2+2\Gamma_-\omega_-)^{1/2}$, $U_\pm(H,T) = \psi(1/2+\hbar\Omega_\pm/2\pi k_B T)-\psi(1/2)$, $\Omega_\pm=\omega_+ + \Gamma_+ \pm \Omega_0$, where $\psi(x)$ is the di-gamma function, and ϕ_0 is the flux quantum. For $\mathbf{H}\|ab$, the in-plane diffusivities in Eq. (1) should be replaced by $[D^{(ab)}D^{(c)}]^{1/2}$.[10] The evolution of $H_{c2}(T)$ and T_c with g is shown in Fig. 3. For dirty π band ($D_\pi \ll D_\sigma$), $H_{c2}(T)$ has an upward curvature at low T, while for dirtier σ band ($D_\pi \gg D_\sigma$) the upward curvature $H_{c2}(T)$ occurs near T_c. Paramagnetic effects can be accounted for by replacing

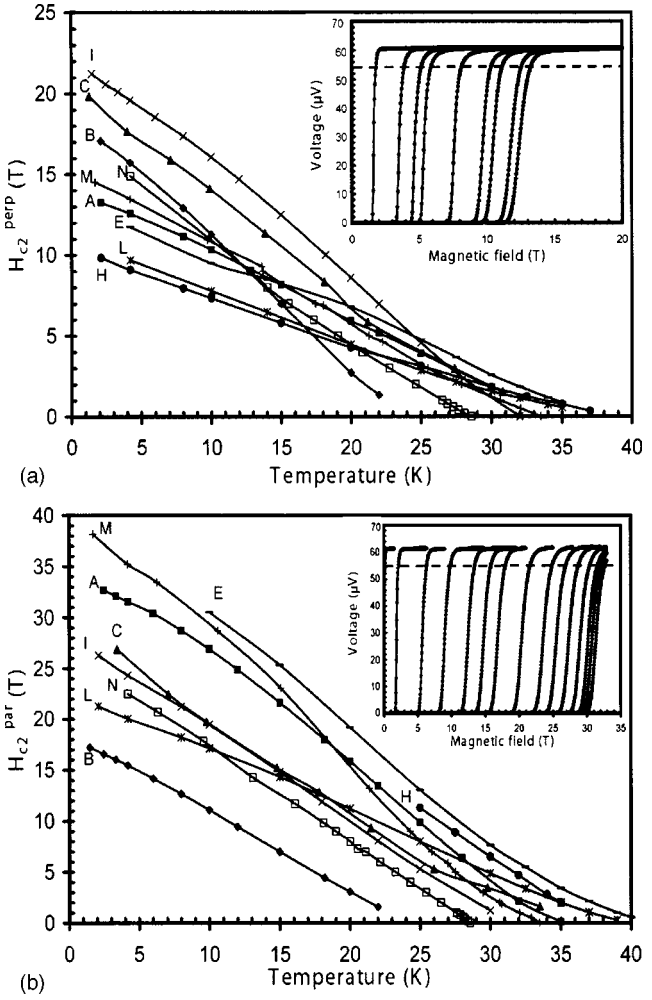

FIG. 1. $H_{c2}{}^{\perp}(T)$ (a) and $H_{c2}{}^{\parallel}(T)$ (b) for samples *A*, *B*, *C*, *E*, *H*, *I*, *L*, *M*, and *N*. The lines are guides for the eye. Insets show $R(H)$ for sample *A* for $T=2.1$, 4.2, 8, 10, 15, 20, 22, 25, 30 K (a), and $T=2.47$, 3.34, 4.2, 6.8, 10, 12, 15, 18.2, 20, 22, 25, 28, 32 K (b). The $R(H_{c2})=0.9R_n$ criterion used to determine H_{c2} is shown as a dashed line.

$\psi(1/2+x)$ with $\mathrm{Re}\psi(1/2+x+i\mu_B H_2 \pi k_B T)$ in Eq. (1), where μ_B is the Bohr magneton.

We used Eqs. (1) and (2) to describe the observed $H_{c2}(T)$, taking *ab initio* values[3] $\lambda_{\sigma\sigma}=0.81$, $\lambda_{\pi\pi}=0.28$, $\lambda_{\sigma\pi}=0.115$, and $\lambda_{\pi\sigma}=0.09$ as input parameters. First, g was calculated from Eq. (2) with the observed T_c and $T_{c0}=39$ K. Next, we calculated D_σ from the observed (or extrapolated) $H_{c2}(0)$, leaving the ratio D_π/D_σ as the only fit parameter determining the shape of $H_{c2}(T)$. This procedure is based on a conventional assumption of the dirty limit theory that impurities only change the scattering rates, but not the coupling constants λ_{mn}, or the partial densities of states N_σ and N_π. Superconductivity in MgB_2 is mostly due to the nearly two-dimensional σ band for which N_σ is weakly dependent of energy, so any small shift of the chemical potential due to doping would not change N_σ. The self-consistency check of this approach is that the shift of T_c due to impurities is weak, and indeed, Eqs. (1) and (2) shows that even if the entire shift of T_c results from changes of N_σ and N_π due to doping, it would have a negligible effect on H_{c2} in our films with $T_c=35-39$ K.

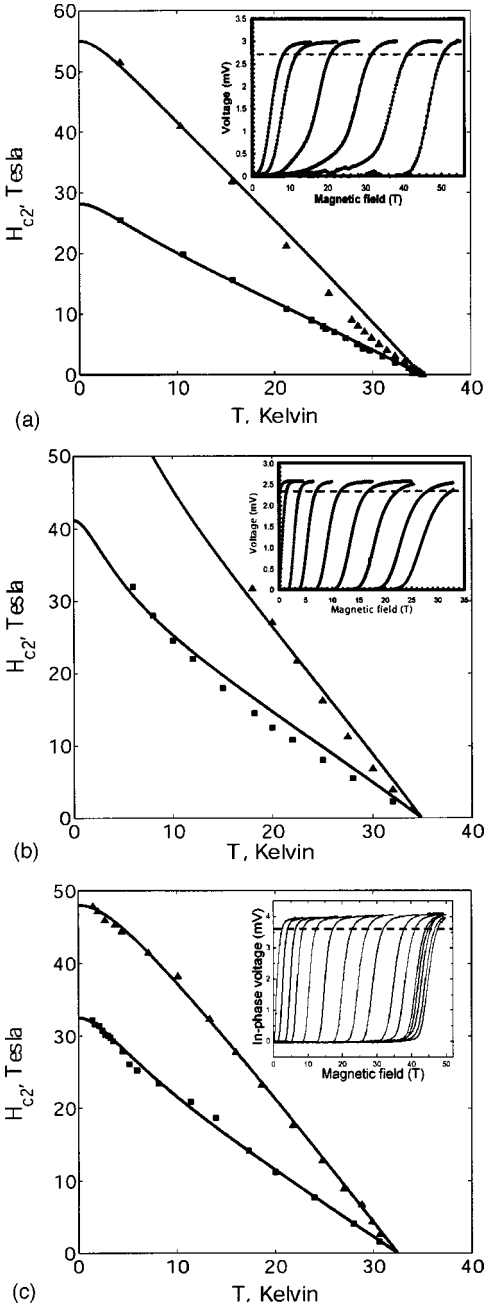

FIG. 2. $H_{c2}{}^{\parallel}(T)$ (triangles) and $H_{c2}{}^{\perp}(T)$ (squares) for films *G* (a), *F* (b), and *D* (c). Insets show the raw $R(H)$ traces for $H\|ab$. Solid curves are calculated from Eqs. (1) and (2) with fit parameters given in Table I.

The fits describe well the observed $H_{c2}(T)$ curves in Fig. 2, indicating that π scattering is stronger than σ scattering in all our high-H_{c2} films. The extrapolated $H_{c2}{}^{\parallel}(0)$ reaches $\approx$55 T for film *G* and $>$70 T for film *F*.[24] Remarkably, the highest H_{c2} values are attained for films with weak T_c suppressions, and the three highest-H_{c2} films [$48<H_{c2}{}^{\parallel}(0)<70$ T] greatly exceed the $H_{c2}{}^{\parallel}(0)$ values reported for C-doped MgB_2 single crystals ($\sim$35 T) (Refs. 25 and 26) and C-doped filaments (32 T).[27] We find that the very broad

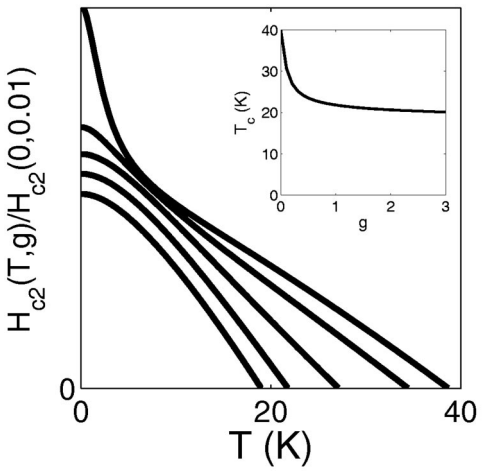

FIG. 3. $H_{c2}(T)$ curves calculated from Eq. (1) for $D_\pi = 0.03 D_\sigma$ and $g = 0.01$, 0.05, 0.2, 1, 10 (from top to bottom). Inset shows $T_c(g)$ calculated from Eq. (2) with λ_{mn} taken from Ref. 3.

range of ρ_n ($\sim 1-600\ \mu\Omega$ cm) does not directly manifest itself in the atomic-scale scattering that actually determines H_{c2}, because current-blocking extended defects[22] control the measured resistivity. TEM on a C-doped HPCVD (Ref. 19) film has shown that a small portion of C is doped into the $Mg(B_{1-x}C_x)_2$ columnar nanograins, which have larger c and a lattice constants than the pure MgB_2. The rest of the C goes into the grain boundaries, consisting of highly resistive amorphous phases. Because T_c is depressed to zero at $x \sim 0.15$ (≈ 10 at. %) and $\rho_n \geqslant 50\ \mu\Omega$ cm in $Mg(B_{1-x}C_x)_2$ single crystals[25,26] and filaments,[27] this would indicate that films with T_c of 33–35 K have $x \sim 0.03-0.05$ within the MgB_2 grains.

As in samples F and G, the c axis is larger than the bulk value in sample D, which shows a high C content as well. TEM study of film D showed buckling of the ab planes[8] (perhaps due to strains induced by as-grown nanophase precipitates), causing the c-axis lattice expansion. Furthermore, lattice buckling results in strong π scattering due to disturbance of the p_z π orbitals, and thus dirtier π band ($D_\pi \ll D_\sigma$) necessary to account for the upward curvature of $H_{c2}(T)$ in Figs. 2(b) and 2(c). In this scenario may also explain how C (which normally substitutes for B) can result both in the strong in-plane σ band scattering and out-of-plane π scattering required for the observed H_{c2} enhancement.

In conclusion, we report extensive studies of the effect of disorder on H_{c2} of MgB_2 and show record high H_{c2} values, which may approach the paramagnetic limit for C-doped multiphase films with a relatively weak T_c suppression.

Work at UW was supported by NSF under MRSEC Grant No. DMR-0079983, work at Penn State was supported under ONR Nos. N00014-00-1-0294 (X.X.X.) and N0014-01-1-0006 (J.M.R.), by NSF under Grants Nos. DMR-0306746 (X.X.X. and J.M.R.), DMR-9876266 and DMR-9972973 (Q.L.), and work at Arizona State University was supported under ONR No. N00014-02-1-0002. The NHMFL user facility is supported by NSF.

[1] A. Y. Liu, I. I. Mazin, and J. Kortus, Phys. Rev. Lett. **87**, 087005 (2001).
[2] H. J. Choi *et al.*, Nature (London) **418**, 758 (2002).
[3] A. A. Golubov *et al.*, J. Phys.: Condens. Matter **14**, 1353 (2002); A. Brinkman *et al.*, Phys. Rev. B **65**, 180517(R) (2002).
[4] P. C. Canfield and G. W. Crabtree, Phys. Today **56**, 34 (2003); P. C. Canfield, S. L. Bud'ko, and D. K. Finnemore, Physica C **385**, 1 (2003).
[5] R. Cava, H. W. Zandbergen, and K. Inumare, Physica C **385**, 8 (2003).
[6] V. Ferrando *et al.*, Phys. Rev. B **68**, 094517 (2003).
[7] F. Bouquet *et al.*, Physica C **385**, 192 (2003).
[8] A. Gurevich *et al.*, Supercond. Sci. Technol. **17**, 278 (2004).
[9] N. R. Werthamer, E. Helfand, and P. C. Hohenberg, Phys. Rev. **147**, 288 (1966).
[10] A. Gurevich, Phys. Rev. B **67**, 184515 (2003).
[11] A. A. Golubov and A. E. Koshelev, Phys. Rev. B **68**, 104503 (2003).
[12] V. Ferrando *et al.*, Supercond. Sci. Technol. **16**, 241 (2003).
[13] C. B. Eom *et al.*, Nature (London) **411**, 558 (2001).
[14] J. Kim *et al.*, IEEE Trans. Appl. Supercond. **13**, 3238 (2003).
[15] X. Zeng *et al.*, Nat. Mater. **1**, 35 (2002).
[16] S. D. Bu *et al.*, Appl. Phys. Lett. **81**, 1851 (2002).
[17] R. Vaglio, M. G. Maglione, and R. Di Capua, Supercond. Sci. Technol. **15**, 1236 (2002).
[18] B. Moeckly (unpublished).
[19] A. V. Pogrebnyakov *et al.*, Appl. Phys. Lett. **85**, 2017 (2004).
[20] R. Gandikota *et al.* (unpublished).
[21] A. V. Pogrebnyakov *et al.*, Appl. Phys. Lett. **82**, 4319 (2003).
[22] J. M. Rowell, Supercond. Sci. Technol. **16**, R17 (2003).
[23] I. I. Mazin *et al.*, Phys. Rev. Lett. **89**, 107002 (2002).
[24] Given the limited field range in our experiments we used Eqs. (1) and (2) without paramagnetic terms. Analysis of paramagnetic effects will be given elsewhere.
[25] T. Masui, S. Lee, and S. Tajima, Phys. Rev. B **70**, 024504 (2004); E. Ohmichi *et al.*, J. Phys. Soc. Jpn. **73**, 2065 (2004).
[26] S. Lee *et al.*, Physica C **397**, 7 (2003).
[27] R. H. T. Wilke *et al.*, Phys. Rev. Lett. **92**, 217003 (2004).